Available online at www.sciencedirect.com
ScienceDirect
Journal of Nuclear Materials 376 (2008) 289–292
journal of nuclear materials
www.elsevier.com/locate/jnucmat

AFM and MFM characterization of oxide layers grown on stainless steels in lead bismuth eutectic

P. Hosemann [a,b,*], M. Hawley [b], G. Mori [a], N. Li [b], S.A. Maloy [b]

[a] CD Laboratory of Localized Corrosion, University of Leoben, Franz-Josef Strasse 18, 8700 Leoben, Austria
[b] Los Alamos National Laboratory, P.O. Box 1663, 87545 Los Alamos, NM, USA

Abstract

Fast reactors and spallation neutron sources may use lead bismuth eutectic (LBE) as a coolant. Its thermal physical and neutronic properties make it a high performance nuclear coolant and spallation target. The main disadvantage of LBE is that it is corrosive to most steels and container materials. Active control of oxygen in LBE will allow the growth of protective oxides on steels to mitigate corrosion. To understand corrosion and oxidation of candidate materials in this environment and to establish a solid scientific basis the surface structure, composition, and properties should be investigated carefully at the smallest scale. Atomic force microscopy (AFM) is a powerful tool to map out properties and structure on surfaces of virtually any material. This paper is a summary of the results from AFM measurements on ferritic/martensitic (HT-9) and austenitic (D9) steels that are candidates for liquid metal cooled reactors.

1. Introduction

Atomic Force Microscopy is a technique introduced by Binning and Rohrer in 1986 [1]. AFM uses a microscopic probe mounted on a low force constant cantilever that is scanned across a sample surface. Short range atomic forces like Van der Waals force are used to detect the surface morphology. Since AFM was first introduced a variety of advanced techniques have been developed, which use specialized probes. It was found that by using tips with specific properties, different sample properties could be mapped. In addition, even though the tip cantilever is designed to exert nano to pico Newton on the sample surface, it was found that if the cantilever was oscillated at its resonance frequency while scanning the surface, one could further minimize surface damage, particularly when imaging soft materials. This technique, however, also allowed one to monitor changes in the resonance frequency due to tip-sample repulsive or attractive interactions. One such technique that evolved is magnetic force microscopy (MFM) [2,3], which utilizes a polarized magnetic tip in a two pass method to detect the topography in the first line scan and the long-range magnetic forces in the second line scan. In the second scan, magnetic data is collected at a fixed height above the surface outside the range of Van der Waals forces. That allows one to simultaneously detect the magnetic structure that correlates one-to-one with the sample surface structure. In this work, AFM/MFM is used to map different topographic features in combination with magnetic properties on oxide layers grown in LBE. This allows insight in the nanoscale structure and the corresponding properties changes which relates to crystallographic and compositional changes.

2. Measurement

We used AFM and MFM to investigate the oxide layers grown on D9 stainless steel (13.6% Cr, 13.6% Ni, 2.1% Mn, 1.11% Mo, 0.85% Si, 0.04% C, 0.30% Ti, balance Fe (by weight)) and HT-9 stainless steel (11.95% Cr, 1% Mo, 0.6% Mn, 0.57% Ni, 0.5% W, 0.4% Si, 0.33% V, 0.2% C,

* Corresponding author. Address: CD Laboratory of Localized Corrosion, University of Leoben, Austria. Tel.: +1 505 606 1437; fax: +1 505 667 7443.
E-mail address: peterh@lanl.gov (P. Hosemann).

0022-3115/$ - see front matter © 2008 Elsevier B.V. All rights reserved.
doi:10.1016/j.jnucmat.2008.02.013

balance Fe (by weight)) in LBE at 535 °C for 3000 h in the IPPE loop in Obninsk, Russia. The oxygen concentration in the LBE was 10^{-6} wt% and the flow rate was 2 m/s. After the samples were exposed to the LBE they were cross sectioned and polished using colloidal silica on a Buehler Vibramet™ as a last polishing step. This final polishing provides a very flat and smooth surface required for AFM measurements. The measurements were carried out using a Veeco Metrology Nanoscope IIIa controller and D3000 microscope. The AFM/MFM tips used for these measurements were commercial silicon Tapping Mode™ cantilevers with magnetic CoCr coated tips (Fig. 1). The scan rate was generally $\leqslant$0.35 Hz for a 40 μm × 40 μm scan area (lower magnification) and adjusted to a higher frequency for higher resolution images. The resonance frequencies of these tips were around 65 kHz.

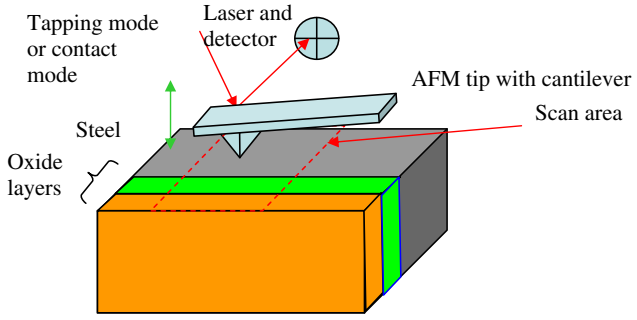

Fig. 1. The setup for performing the AFM and MFM measurements on the oxide layers on steels formed in LBE.

3. Results

Both materials showed a multi-layer structure as previously reported in the literature by SEM (scanning electron microscopy) analyses [4]. AFM/MFM characterization allows a much more detailed grain and microstructure analysis than SEM allows. In the topographic image bright colors are high structures while dark colors are low structures. Since grains of different orientations polish at slightly different rates the grains can be visualized. In the magnetic force image strong contrasts (dark and bright colors) mean a strong magnetic polarization while weak contrasts mean a weak magnetic field. MFM can not detect transverse magnetic fields. Here, MFM is used to visualize magnetic structural changes as a indicator for compositional or crystallographic changes in the oxide layers and AFM is used to visualize the micro structure.

Fig. 2 shows the AFM/MFM images from a D9 sample. It can be seen that there are two outer magnetic layers, which differ in their grain structure but both show many large pores. The magnetic structure correlates with the grain structure and compositional differences. It is reported in the literature [4,5] that the outer layer is magnetite (Fe_3O_4). We found that the outer layer has a strong magnetic structure. It has been reported that Cr rich spinels ($FeCr_2O_4$) are antiferromangetic with a $T_C = 473$ °C and no magnetic moment while Fe rich spinels (Fe_3O_4) are ferromagnetic with a T_N of 860 °C and a magnetic moment of 3.47 μB and Fe_2NiO_4 is ferromag-

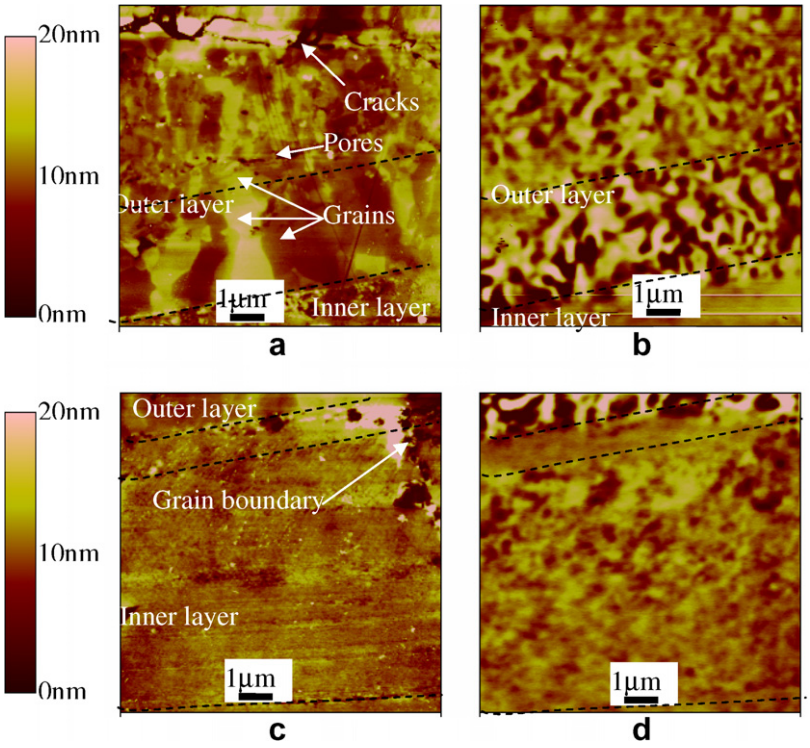

Fig. 2. The AFM (left images (a) and (c)) and the MFM (right images (b) and (d)) results on the oxide layers formed on the D9 steel. Figure (a) and (b) present the images located at the outer oxide layer while figure (c) and (d) present images located at the inner oxide layer.

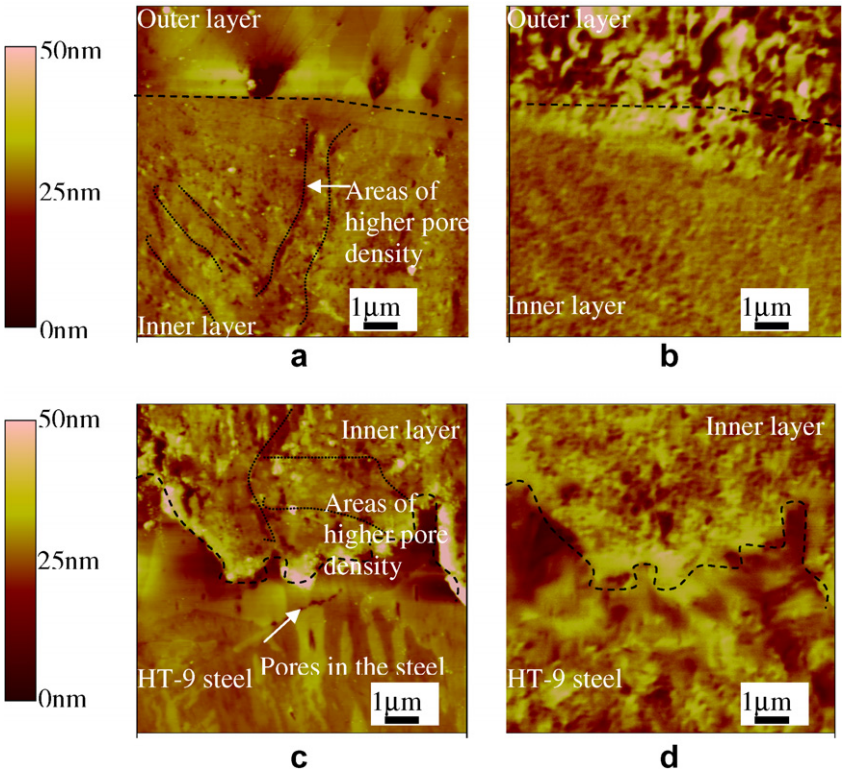

Fig. 3. The AFM (left images (a) and (c)) and the MFM (right images (b) and (d)) results on the oxide layers formed on the HT-9 steel. Figure (a) and (b) present the images located at the outer oxide layer while figure (c) and (d) present images located at the inner oxide layer.

netic with a magnetic moment of 1.5–2.4 μB [6]. Spinels with a composition changing from $FeCr_2O_4$ to Fe_3O_4 have increasingly strong magnetic properties [7]. It is assumed that the outer layer is indeed magnetite since it has the strongest magnetic moment according to the literature and it was measured as such. In the outer layer two different grain size areas are found. The outer most area within the outer layer appears to have smaller grains (120–400 nm grain size) than the inner area (0.8–3.5 μm). The inner oxide layer shows similar grain boundaries to those in the bulk steel. To verify that these boundaries are indeed the original steel grain boundaries more analysis will be needed. Its magnetic signal is weaker than the signal of the outer layer therefore it is assumed it is Ni and Cr enriched versus the outer layer. There is a thin (<1 μm) region between the outer and inner layers where the magnetic structure disappears. The exact corresponding composition of this thin layer is not presently known. But based on the weak magnetic signal it is assumed that this thin (1 μm) layer is relatively Cr rich. The outer layer thickness is 5–20 μm while the inner layer is 5–10 μm thick.

Fig. 3 are AFM/MFM images of HT-9. A multiple oxide layer structure similar to what is reported in the literature [4] was found. The outer layers show a strong magnetic structure, which suggests that this is magnetite. The outer layer shows many large pores and a strong magnetic response. It can be also seen that the grain structure is very similar to the grains structure found in D9. In contrast, the inner layer shows a weaker magnetic response than in D9 which is most likely due to the fact that no Ni is present in this material. There was no non-magnetic layer detected between the inner and outer layers. The inner layer has a very large amount of pores that are connected and seem to outline grains and a martensitic lath structure. In some areas pores within the steel close to the inner oxide layer located at the steel grain boundaries were found as well. This leads to the assumption that the pores in the inner oxide layer are the former steel grains. More detailed AFM/MFM and TEM measurements and analysis are needed to reveal more details and to confirm this interpretation. The outer layer thickness is 6–8 μm while the inner layer is 10–12 μm thick.

4. Conclusion and summary

- It is possible to detect the multi layer oxide structure on HT-9 and D9 stainless steel due to oxidation in LBE using the AFM and MFM techniques. AFM/MFM techniques can be used to measure large areas of interest and their relative property changes (magnetic properties) which indicate local changes in composition and structure.
- The outer layer on both materials (HT-9 and D9) is highly magnetic consistent with a magnetite composition as previously reported in the literature.

- The inner layer has a weaker magnetic response than the outer layer, and it appears that large amount of defects (pores and particle) develop at the grain boundaries in the steel.

References

[1] G. Binning, C.F. Quate, Ch. Gerber, Phys. Ref. Lett. 56 (9) (1986) 930.
[2] Y. Martin, H.K. Wikramashinge, Appl. Phys. Lett. 50 (1987) 20.
[3] J.J. Saenz, N. Garcia, P. Gruetter, E. Meyer, H. Heinzelmann, R. Wiesendanger, L. Rosenthaler, H.R. Hidber, H.J. Guentherodt, J. Appl. Phys. 62 (10) (1987) 4293.
[4] H. Glasbrenner, J. Konys, G. Mueller, A. Rusanov, J. Nucl. Mater. 296 (2001) 1.
[5] J. Zhang, N. Li, Y. Chen, A.E. Rusanov, J. Nucl. Mater. 336 (2005) 1.
[6] H. Perron, T. Mellier, C. Domain, J. Roques, E. Simoni, R. Drot, H. Catalette, J. Phys.: Condens. Matter. 19 (2007) 10.
[7] V. Halpern, Proc. Roy. Soc. London Series A, Math. Phys. Sci. 291 (1966) 113.